Carbon Letters (2024) 34:529–536
https://doi.org/10.1007/s42823-023-00599-9

Online ISSN 2233-4998
Print ISSN 1976-4251

ORIGINAL ARTICLE

Achievement of an efficient oxygen reduction electrocatalyst based on carbon boosted with $MnO_x/MnCo_2O_4$ with excellent electrocatalytic activity in neutral media

Masoumeh Ghalkhani[1] · **Rasol Abdullah Mirzaie**[2] · **Fatemeh Shahmoradi**[1,2] · **Azam Anaraki Firooz**[2]

Received: 13 April 2023 / Revised: 24 July 2023 / Accepted: 24 August 2023 / Published online: 5 September 2023
© The Author(s), under exclusive licence to Korean Carbon Society 2023

Abstract

In the current research, a manganese and cobalt oxides-based nanocatalyst was developed which was used to make an efficient cathode electrode for fuel cells. The nano $MnO_x/MnCo_2O_4$ was synthesized through a hydrothermal procedure followed by sintering at 500–600 °C. X-ray diffraction and scanning electron microscopy besides electrochemical techniques were applied for the characterization of the synthesized nanocatalyst. The carbon black type Vulcan (XC-72R) and PTFE were used to prepare the active reaction material of the cathode electrode named carbon paste (CP). Loading of the synthesized nano $MnO_x/MnCo_2O_4$ on CP was optimized in a weight ratio of 10–90% for the oxygen reduction process in neutral conditions. The best performance was gained for the 50 W% $MnO_x/MnCo_2O_4$ loaded CP, whose active surface area was twice the bare CP. The values of the exchange current density of the ORR obtained by electrode containing 50 W% $MnO_x/MnCo_2O_4$ was calculated as 0.12 mA/cm^2. The low price, good catalytic efficiency, and cyclic stability of the $MnO_x/MnCo_2O_4$ nanocatalyst compared to the commercial platinum-based catalysts confirm its ability to develop fuel cell electrodes.

Keywords Fuel cell · Oxygen reduction reaction · Catalyst · Manganese oxide · Cobalt oxide

1 Introduction

The urgent need for energy to promote industrial and technological development and to prevent environmental degradation has led the majority of scientific research in the direction of sustainable development. Production and storage of electricity with the help of green approaches independent of fossil fuels can be an efficient solution [1]. Oxygen reduction and water-splitting reactions are two main processes in this field [2–5]. Since the only and main cathode process in fuel cells is the oxygen reduction reaction (ORR), it is called the heart of the fuel cell [6]. Although the materials required for these processes are easily available, the non-spontaneity of these reactions and the high activation energy required are serious limitations in this direction [7, 8].

The oxygen reduction reaction, especially in neutral environments, is of interest to energy researchers because it is a critical process in biofuel cells. Oxygen reduction in neutral media is kinetically slow. To facilitate this reaction and increase the efficiency of the fuel cell, it is necessary to use a suitable electrocatalyst. The development of efficient electrocatalysts is very effective in facilitating these processes [2, 8]. In recent years, researchers have been looking for inexpensive alternatives to non-precious metals as catalysts to have an activity equal to or greater than platinum, and also have a longer life and stability [9–11].

Although various electrocatalysts have been introduced, limitations such as the lack of stability of the modifiers, high cost, and low energy density have hindered the global development of clean energy production systems based on oxygen reduction reaction (ORR) [12]. A wide range of electrocatalysts based on transition metals and their oxides/composites have been developed to boost the ORR [13–15]. Unfortunately, the catalytic activity of transition metal oxides alone

---

✉ Masoumeh Ghalkhani
ghalkhani@sru.ac.ir

✉ Rasol Abdullah Mirzaie
ra.mirzaei@sru.ac.ir

[1] Electrochemical Sensors Research Laboratory, Department of Chemistry, Faculty of Science, Shahid Rajaee Teacher Training University, Lavizan, P.O. Box 1678815811, Tehran, Iran

[2] Fuel Cell Research Laboratory, Department of Chemistry, Faculty of Science, Shahid Rajaee Teacher Training University, Lavizan, P.O. Box 1678815811, Tehran, Iran

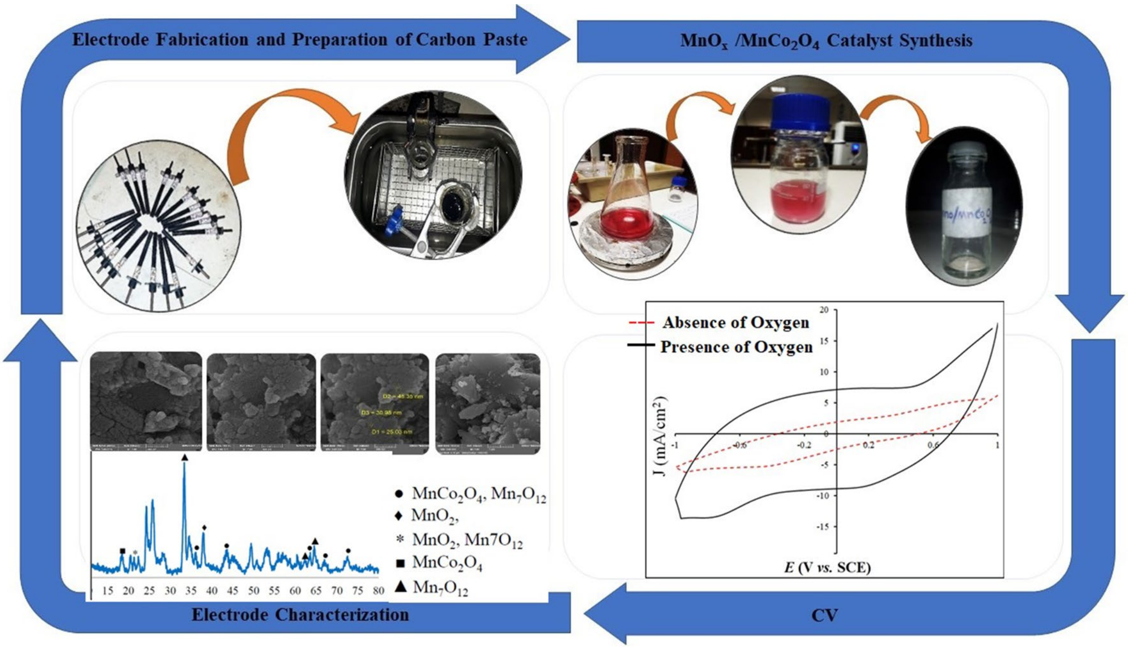

Scheme 1. The schematic presentation of the electrocatalyst synthesis, electrode preparation and its usage for ORR process

is low compared to noble metals and needs to be boosted [16]. On the other hand, the problem of corrosion and oxidation phenomena prevents their satisfactory electrocatalytic activity and hinders their use in making practical fuel cell electrodes [6, 17]. The construction of non-noble metal-based electrocatalysts with proper ORR activity and low production cost is the main challenge in the research field of fuel cells [18]. The use of hybrid and composite nanostructures of transition metals with other active electrocatalytic compounds can significantly improve their performance, especially their long-term stability [17, 19].

Non-precious metal oxides of Ni [20, 21], Co [22–24], Mn [25, 26], and Fe [27, 28] were extensively developed to overcome charge transfer restrictions and to extend the electrode stability. These compounds are more available and abundant, and more importantly, they are eco-friendly. The use of manganese dioxide in the development of electrocatalysts is not only in line with the principles of sustainable development and reduces the total price, but also brings the benefits of a wide active surface area and high specific capacity [29–31]. Therefore, it has been given a lot of attention. On the other hand, low electronic conductivity and cyclic stability are the main limitations of this metal oxide [30, 32]. To solve this problem, effective compounds such as cobalt oxide, which has high conductivity and suitable electrocatalytic properties, can be used [30, 33]. Till now, researchers have introduced diverse compounds to improve the electrocatalytic process of oxygen reduction. To boost the electrocatalytic performance of MnO_2 for ORR, composites such as Mn_3O_4/CoO [34], $MnO_2/NiCo_2O_4$ [35], MnO_2/TiO_2 [36], MnO_2/Fe_2O_3 [37], $MnO_2@Co_3O_4$ [38], and MnO_2-CNTs/Co_3O_4 [39] have been prepared. The synergetic impact of the individual constituents of the nanocomposites led to the appearance of satisfied catalytic features [40–43].

Considering the prominent and proven characteristic of manganese oxide to catalyze the electrochemical ORR, in the present work, we focused on the development of an efficient catalyst based on manganese oxide, Scheme 1. Here, an efficient ORR catalyst based on a composite of nano MnOx and $MnCo_2O_4$ is introduced. It has been reported that spinel $MnCo_2O_4$ shows higher electronic conductivity than MnO_2 and Co_3O_4. So, to solve the problem of low stability and low electrical conductivity of manganese oxide, spinel $MnCo_2O_4$ was used. It should be noted that carbon-based nanostructures have been commonly used to improve the stability and electrical conductivity of manganese oxide, but in current work, we have only used metal oxides. Another difference between the present work and previous reports is the use of neutral solution instead of an alkaline solution for ORR evaluations. We focused on the construction of electrodes based on Mn–Co oxides composites for ORR. The parameters involved in the electrocatalytic process of oxygen reduction were evaluated and optimized. The catalytic performance of electrodes relied on the composition of the components and their weight percentage in the texture of the electrode active layer.

2 Experimental

2.1 Chemicals and materials

Carbon black powder (Vulcan XC-72 R), polytetrafluoroethylene (PTFE-Aldrich 96%), isopropanol (Merk), $Mn(NO_3)_2{\cdot}2H_2O$, and $Co(NO_3)_2{\cdot}6H_2O$ were supplied from Sigma-Aldrich Co. All chemical materials were utilized as received without further purification.

2.2 Synthesis of $MnO_x/MnCo_2O_4$ nanocatalyst

The hydrothermal method was employed for the nanocatalyst synthesis. 5 mmol $Mn(NO_3)_2{\cdot}2H_2O$ and 5 mmol $Co(NO_3)_2{\cdot}6H_2O$ were added to an Erlenmeyer flask containing a 40 mL solution of the EtOH and ethylene glycol (with a ratio of 3:1). The content of the Erlenmeyer flask was stirred using a magnetic stirrer for 30 min. Then, the solution was purred in an autoclave that was placed in an oven and heated at 110 °C for 24 h. The content of the Erlenmeyer flask was filtered through filter paper. The obtained precipitate was washed with D.I. water and EtOH and left to dry in the laboratory environment. Finally, the resulting powder was sintered in the oven at a temperature of about 500–600 °C for 50 min. The synthesized nanocatalyst was named as $MnO_x/MnCo_2O_{4.}$

2.3 Electrode construction

Here, the graphite rods ($r = 3.5$ mm) taken from the disposable batteries were utilized as an electrode substrate. The graphite rods were acid washed, and then rinsed with deionized water and dried in an oven at 60 °C. The lateral surface of the graphite rods was thoroughly covered with parafilm, which left only its cross section with 0.38 cm^2 surface area exposed to the solution. The active reaction material of the electrode was prepared using carbon black type Vulcan (XC-72R), PTFE, isopropanol, and D.I. water as solvent. The prepared suspension was transferred to the oven and let the solvent was evaporated at 100 °C, until formed a sticky paste. This material was named CP. The optimum time of remaining the electrode material in the oven was determined as 5 min. To fabricate modified CPs, the synthesized nano $MnO_x/MnCo_2O_4$ was added to the carbon Vulcan–PTFE mixture in various ratio percentages of 10–90% (to optimize the $MnO_x/MnCo_2O_4$ value). The electrodes were prepared by covering the cross section of the graphite rods with a thin film of 10 mg of the prepared bare CP or CP-$MnO_x/MnCo_2O_4$. The final electrodes were named GE (substrate), GE/CP (bare electrode), and GE/CP-$MnO_x/MnCo_2O_4$ (modified electrode).

2.4 Physical and electrochemical investigations

The crystalline structure of the prepared $MnO_x/MnCo_2O_4$ nano compound was evaluated with X-ray diffraction (XRD) analysis (PHILIPS-PW1730, Netherlands, the radiation of CuKα, $\lambda = 1.5418$ Å). The $MnO_x/MnCo_2O_4$ morphology was characterized by scanning electron microscopy (SEM, TESCAN-MIRA III made in the Czech Republic).

A three-electrode cell assembly connected to potentiostat–galvanostat (BHP, Model 2083, Iran) was utilized for voltammetric experiments (linear sweep and cyclic voltammetry: LSV and CV, respectively) at room temperature. The ORR performance and stability tests were done in an O_2 (or N_2)-saturated 0.1 M phosphate buffer solution (PBS, pH 7.0). A graphite rod (bare or modified), a platinum wire, and a saturated calomel electrode (SCE) were used as the working, counter, and reference electrodes, respectively. The electrochemical impedance spectroscopy (EIS) tests were performed utilizing a single-channel potentiostat Origalys (OrigaFlex-OGF500).

3 Results and discussion

3.1 Characterization of the $MnO_x/MnCo_2O_4$ nano electrocatalyst

The XRD pattern for $MnO_x/MnCo_2O_4$ is shown in Fig. 1. In this figure, the presence of $MnO_x/MnCo_2O_4$ peaks confirms the formation of this composite. Each of $2\theta = 18.5$, 21, 33, 36, 38, 44, 57, 62, 64, 65, 67, 73 in the XRD pattern of the $MnO_x/MnCo_2O_4$ nanocomposite corresponds to manganese oxides with different oxidation numbers and $MnCo_2O_4$. Each of these peaks is related to plates 1, 2, and 3, respectively, which are reported according to sources. The different oxidation states of manganese oxides can be attributed to the presence of MnO, Mn_2O_3, and MnO_2 in the composite, while

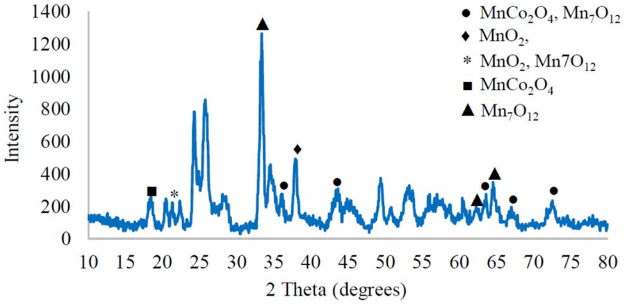

Fig. 1 XRD pattern of $MnO_x/MnCo_2O_4$

$MnCo_2O_4$ corresponds to the spinel structure of the composite. The crystal structure can also affect the electronic properties of the composite. The electronic properties can influence the charge transfer kinetics and the efficiency of the electron transfer between the electrode and the reactants.

The morphology of $MnO_x/MnCo_2O_4$ nanocomposites was investigated using FE-SEM. The images with 200 Kx magnification are shown in Fig. 2. The prepared nanocomposites are accumulated next to each other in the form of spherical nanoparticles. This nanocomposite has a non-uniform particle size with an average particle size between 25 and 40 nm. The morphology of the nanocomposite is an important factor that can affect its electrocatalytic performance. The high surface area to volume ratio of the spherical nanoparticles can provide more active sites for electrocatalytic reactions. The non-uniform particle size can also create defects and exposed crystal planes, which can enhance the catalytic activity of the nanocomposite. However, the non-uniform particle size can also lead to aggregation and decrease the overall stability of the nanocomposite.

3.2 Electrochemical studies

The voltammetric response of the electrodes prepared in the same procedure named GE/CP (bare electrode), and GE/CP-$MnO_x/MnCo_2O_4$ (modified electrode) was evaluated. The wide potential range of – 1.0 to 1.0 V, a potential sweep rate of 100 mV/s, and a phosphate buffer solution (PBS, pH 7.0) saturated with O_2 (for the presence of oxygen) or N_2 (for the absence of oxygen) were chosen as experiments conditions, Fig. 3. The CVs of the GE/CP were almost the same in the presence and absence of oxygen, Fig. 3a, revealing the

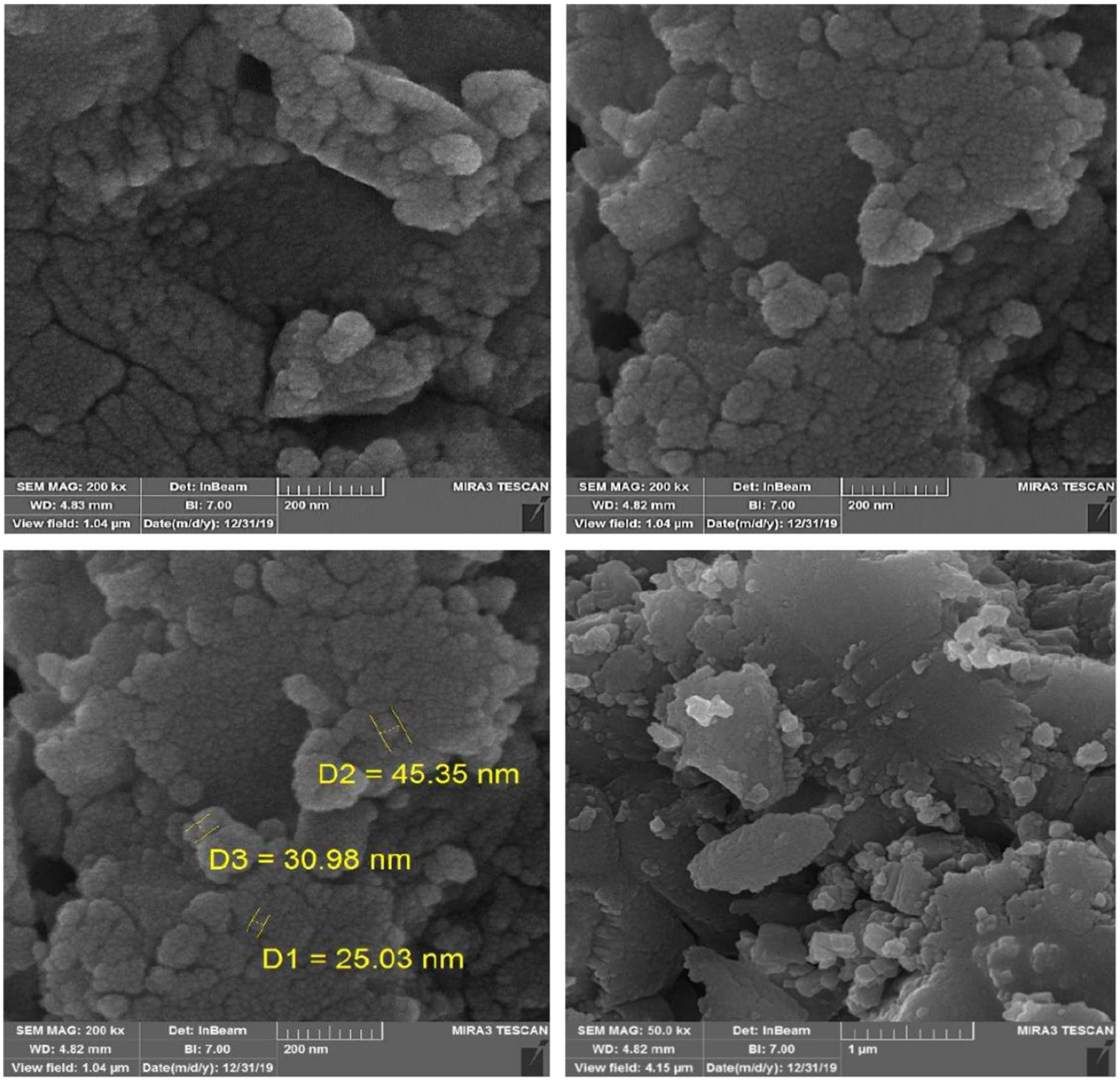

Fig. 2 FE-SEM image of $MnO_x/MnCo_2O_4$

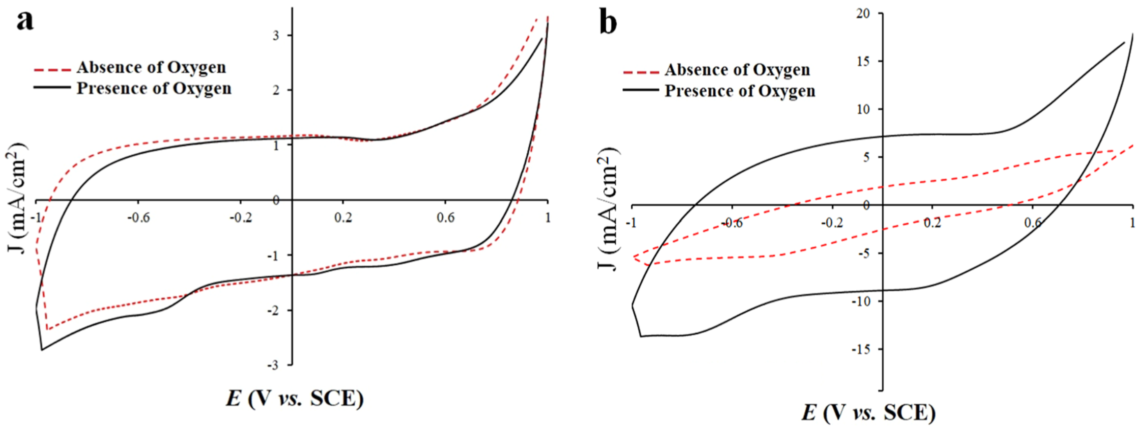

Fig. 3 CVs of **a** GE/CP and **b** GE/CP-$MnO_x/MnCo_2O_4$ in PBS, pH 7.0 in the presence and absence of oxygen

insensitivity of the bare electrode to the oxygen molecules. The recorded CV by GE/CP did not show any peak in the N_2-saturated PBS. However, when oxygen enters the cell, a very tiny reduction peak appeared at a potential of − 0.5 V. The current intensity was also very small for this reduction peak, so it can be concluded that the GE/CP does not have a good ability to electrochemically reduce oxygen molecules.

The CV current in PBS was increased when the surface of GE/CP was modified by $MnO_x/MnCo_2O_4$ nanocomposite probably due to the enhancement of electrode conductivity and electrochemically active surface area, Fig. 3b. No peak was observed for GE/CP-$MnO_x/MnCo_2O_4$ in the absence of oxygen. The presence of oxygen in the solution made a sensible change in the CV response of GE/CP-$MnO_x/MnCo_2O_4$ confirming the appearance of the electrocatalytic behavior for ORR. In fact, the $MnO_x/MnCo_2O_4$ nanocomposite with active catalytic sites can catalyze the ORR and its high surface area provides numerous catalytic sites, thus increasing the rate of oxygen depletion through ORR and, thus, oxygen reduction current.

A series of GE/CP-$MnO_x/MnCo_2O_4$ were constructed utilizing different values of the modifier to optimize $MnO_x/MnCo_2O_4$ percentage in the electro-active layer of the electrode. Figure 4 displays recorded CVs of these electrodes swept from − 1.0 to + 1.0 V (vs. SCE) at a sweep rate of 100 mV/s in 0.01 M PBS saturated with O_2. The presence of $MnO_x/MnCo_2O_4$ nanocomposite made possible the ORR in positive potentials. An obvious shift of the open circuit voltage (OCV) of ORR to about 0.7 V reveals the fast process with very low kinetic restrictions. The best response was gained for the GE modified with 50 W% CP and 50 W% $MnO_x/MnCo_2O_4$ (CP50-$MnO_x/MnCo_2O_4$50).

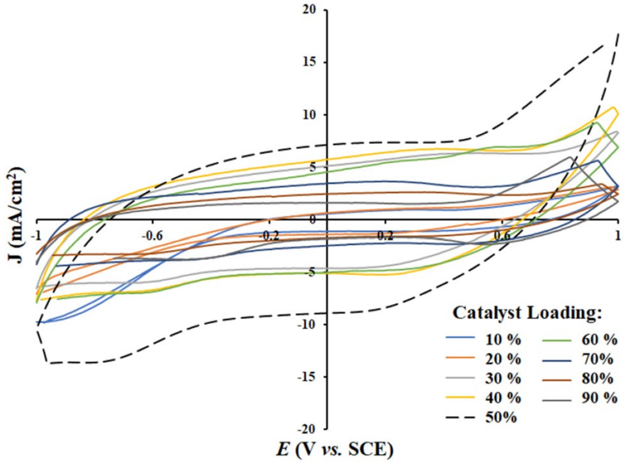

Fig. 4 CVs of GE modified with various W% of $MnO_x/MnCo_2O_4$ catalyst and CP recorded in O_2-saturated PBS, pH 7.0 at a scan rate of 100 mV/s

The optimization of the electrode is critical to achieving higher ORR electrocatalytic activity. In fact, the GE/CP50-$MnO_x/MnCo_2O_4$50 provided a better catalytic effect for ORR than other amounts of the nanocomposite. The value of the CP controls the electrode conductivity and porosity of the electrode material that facilitates the reactant transfer toward the electrode surface and quickly removes the products of the electrochemical reactions from the electrode surface. Here, the $MnO_x/MnCo_2O_4$ percentage affects the electrocatalytic impact so the current density of the ORR and its OCV. In the presence of 50% of $MnO_x/MnCo_2O_4$ nanocomposite, more electro-active species are involved in ORR. However, utilizing more than 50 W% nanocatalyst in the modification step caused the surface of the electrode to be blocked and the conductivity of the electrode surface to be reduced; thus, the efficiency of the ORR was attenuated. Therefore, the GE surface was modified with the CP50-$MnO_x/MnCo_2O_4$50 as the optimum composite to achieve higher ORR electrocatalytic activity.

For the kinetic study of ORR at neutral media, the linear sweep voltammogram (LSV) tests in O_2-saturated PBS, pH

7.0, at a scan rate of 1 mV/s were performed to get the Tafel plot. In the case of the observed peak for ORR at – 0.04 V, the high slope of the plot of current *vs.* potential, in the interval of the starting point of the Faraday current to the peak current (+ 0.12 to – 0.04 V), indicates that the reaction is kinetically fast and desirable without any kinetic limitation. Based on the plot of the current logarithm *vs.* the overvoltage, the exchange current density for the GE modified with CP50-MnO_x/$MnCo_2O_4$50 under optimized situation was obtained at 0.12 mA cm^{-2}. That indicates the ORR at GE/CP50-MnO_x/$MnCo_2O_4$50 is kinetically fast in neutral media. These results suggest that the electrode has a high efficiency for the ORR, which is a critical factor in fuel cells and other electrochemical applications.

Electrochemical impedance spectroscopy was used to evaluate the GE/CP modified with MnO_x/$MnCo_2O_4$ nanocomposite (50%) at various voltages, Fig. 5. An equivalent circuit is proposed according to the impedance behavior in Fig. 5. In this circuit, the parameters can be described as: R_1: solution resistance, C: capacitance of the dielectric layer, R_2: charge transfer resistance, and W: Warburg element. The parameters of the equivalent circuit were calculated (Table 1) by fitting the model to the electrochemical impedance data. Table 1 indicates that the capacity of the double layer decreases concerning the maximum current density, which leads to a slight increase in the resistance related to species diffusion to the electrode surface. On the other hand, reducing the potential from the value of the OCV led to a decrease in the resistance to charge transfer (R_2), which is a beneficial condition for a higher rate of the ORR at the peak potential. The decrease in capacitance of the double layer with increasing current density indicates that the oxygen concentration at the electrode surface is depleted as the ORR proceeds. This suggests that the ORR rate can be further improved by increasing the oxygen concentration at the electrode surface, possibly by increasing the oxygen flow rate or by optimizing the electrode design to enhance oxygen mass transport.

Table 1 The best-fit impedance parameters of the GE/CP50-MnO_x/$MnCo_2O_4$50 at various potentials

Potential	Resistance (R_1)/ Ohm	Capacitance/ (C) 10^{-6} F	Resistance (R_2)/ Ohm	Warburg/ (W) Ohm
OCV	82.76	9.9792	17.02	30.33
Peak potential	74.56	5.3881	15.34	31.71

The surface area of the GE/CP and the GC/CP50-MnO_x/$MnCo_2O_4$50 was obtained using the Randles–Sevcik equation from the slope of the current diagram versus the square of the scan rate in the electrochemical probe solution. The calculated surface areas were 24.69 and 49.38 cm^2, respectively. The electrode surface area was extended after introducing MnO_x/$MnCo_2O_4$ nanocatalyst. The increase in surface area can lead to a higher response for ORR, as there is more surface available for the reaction to occur. This can improve the electrocatalytic activity of the electrode and enhance the ORR performance. In addition, the higher surface area can also improve the mass transport of reactants and products to and from the electrode surface, which can further enhance the ORR performance. This is because a higher surface area provides more sites for reactants to adsorb and more pathways for the transport of products away from the electrode surface. Therefore, the increase in surface area due to the introduction of the MnO_x/$MnCo_2O_4$ nanocatalyst can enhance not only the electrocatalytic activity but also the mass transport properties of the electrode.

The stability of the GC/CP50-MnO_x/$MnCo_2O_4$50 was evaluated by the CV technique. The successive CVs in a PBS, pH 7.0, purged with oxygen gas were recorded in the potential window of 1.0 to – 1.0 V at a scan rate of 100 mV/s. After 200 CV runs no obvious variation appeared

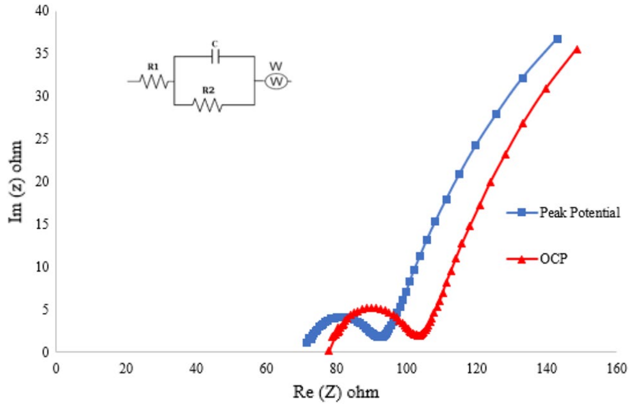

Fig. 5 Nyquist diagrams of the GE/CP50-MnO_x/$MnCo_2O_4$50 in the PBS with pH 7 in the frequency range of 100 kHz–0.1 Hz, at different voltages

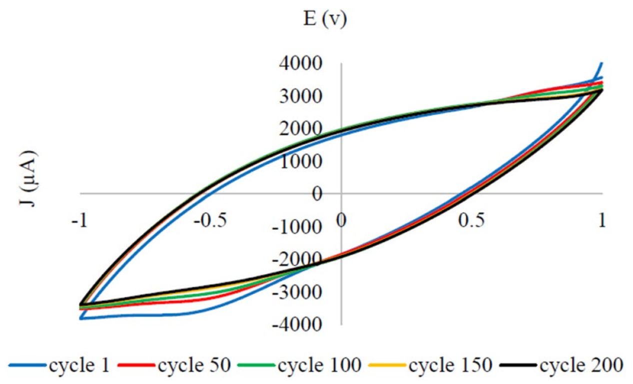

Fig. 6 Consecutive voltammograms of the GC/CP50-MnO_x/$MnCo_2O_4$50 recorded in PBS, pH 7.0 at scan rate of 100 mV/s

in the CV response of GC/CP50-$MnO_x/MnCo_2O_4$50. Some CVs depicted in Fig. 6 reveal the good maintenance of the electrocatalytic activity of the constructed electrode toward ORR. This is a promising result for practical applications, as it suggests that the electrode is durable and reliable. This can be useful in designing ORR systems that require long-term operation and reliability.

4 Conclusions

Electrocatalysis is an important field of study due to its potential applications in various fields, including energy conversion and storage. In this research, the electrocatalytic activity of the $MnO_x/MnCo_2O_4$ electrocatalyst was evaluated in a neutral environment for ORR. The ORR is a crucial process in many electrochemical devices, including fuel cells, metal-air batteries, and air–cathode microbial fuel cells. The ORR current density can be significantly influenced by the percentage of $MnO_x/MnCo_2O_4$ in the electro-active layer of the electrode. Therefore, it is important to optimize the $MnO_x/MnCo_2O_4$-based modified electrode's composition to increase the oxygen reduction rate. The nano $MnO_x/MnCo_2O_4$ offers numerous catalytic active sites, which provide a high surface area for the ORR to take place. The number of active sites available for the ORR is directly proportional to the reaction rate. The presence of MnO, Mn_2O_3, and MnO_2 with varying oxidation states contribute to these active sites, providing different redox potentials that facilitate the ORR. The spinel structure of $MnCo_2O_4$ can also enhance the catalytic activity by providing a suitable crystal structure for the adsorption and activation of oxygen molecules. The high surface area of the $MnO_x/MnCo_2O_4$ nanocomposite provides numerous catalytic sites, increasing the reaction rate and reducing the overpotential for ORR. The nanocomposite can enhance the electron transfer kinetics by providing a conductive pathway for the electrons to reach the active sites. The morphology and crystal structure of the $MnO_x/MnCo_2O_4$ nanocomposite can also affect the electrocatalytic behavior by influencing the diffusion properties and accessibility of the active sites. In conclusion, the results of this study suggest that the $MnO_x/MnCo_2O_4$ composite material is a suitable candidate for use as a fuel cell electrocatalyst for ORR in neutral media. This research provides valuable insights into the development of efficient and effective electrocatalysts for fuel cells, which are crucial for the advancement of clean energy technologies.

Acknowledgements The authors gratefully acknowledge the support of this work by the Shahid Rajaee Teacher Training University, I.R. Iran under grant 5037. In addition, the authors would like to acknowledge the support of the Fuel Cell Research Laboratory (FCRL) of Shahid Rajaee Teacher Training University (Tehran, Iran).

Data availability Data available on request from the authors.

Declarations

Conflict of interest The authors declare that they have no conflict of interest.

References

1. Moeini B, Avval TG, Linford MR, Ghalkhani M, Kaykhaii M, Mirzaie RA (2021) Surface-orientated platinum nanoparticles electrodeposited on a carbon substrate as a high performance electrocatalyst for glucose oxidation reaction in alkaline media. Mater Sci Eng B 268:115147
2. Wu Y, Ghalkhani M, Afshar EA, Karimi F, Xia C, Van Le Q, Vasseghian Y (2022) Recent progress in biomass-derived nanoelectrocatalysts for the sustainable energy development. Fuel 323:124349
3. Khademi D, Zargazi M, Chahkandi M, Baghayeri M (2023) A novel γ-BMO@BMWO Z-scheme heterojunction for promotion photocatalytic performance: nanofibers thin film by co-axial-electrospun. Environ Res 219:115154
4. Zargazi M, Chahkandi M, Mahdi Baghayeri M (2022) New highly efficient 2D/1D HAp/g-C_3N_4 photocatalyst thin film insight into crystal orientation and C-vacancy effects. Chemosphere 303:135079
5. Mehrkhah R, Mohammadi M, Zenhari A, Baghayeri M, RezaeeR-oknabadi M (2023) Antibacterial evaporator based on wood-reduced graphene oxide/titanium oxide nanocomposite for long-term and highly efficient solar-driven wastewater treatment. Ind Eng Chem Res 62:4573–4586
6. Ahmed MS, Choi B, Kim Y-B (2018) Development of highly active bifunctional electrocatalyst using Co_3O_4 on carbon nanotubes for oxygen reduction and oxygen evolution. Sci Rep 8(1):1–10
7. Sohrabi S, Dehghanpour S, Ghalkhani M (2016) Three-dimensional metal–organic framework graphene nanocomposite as a highly efficient and stable electrocatalyst for the oxygen reduction reaction in acidic media. ChemCatChem 8(14):2356–2366
8. Sohrabi S, Ghalkhani M (2019) Metal–organic frameworks as electro-catalysts for oxygen reduction reaction in electrochemical technologies. J Electron Mater 48(7):4127–4137
9. Baghayeri M, Ansari R, Nodehi M, Veisi H (2018) Designing and fabrication of a novel gold nanocomposite structure: application in electrochemical sensing of bisphenol A. Int J Environ Anal Chem 98:874–888
10. Nodehi M, Baghayeri M, Behazin R, Veisi H (2021) Electrochemical aptasensor of bisphenol A constructed based on 3D mesoporous structural SBA-15-Met with a thin layer of gold nanoparticles. Microchem J 162:105825
11. Baghayeri M, Nodehi M, Amiri A, Amirzadeh N, Behazin R, Iqbal MZ (2020) Electrode designed with a nanocomposite film of CuO honeycombs/Ag nanoparticles electrogenerated on a magnetic platform as an amperometric glucose sensor. Anal Chim Acta 1111:49–59
12. Sohrabi S, Ghalkhani M, Dehghanpour S (2019) The electrocatalytic stability investigation of a proton manager MOF for the oxygen reduction reaction in acidic media. J Inorg Organomet Polym Mater 29(2):528–534
13. Ibrahim KB, Tsai MC, Chala SA, Berihun MK, Kahsay AW, Berhe TA, Su WN, Hwang BJ (2019) A review of transition metal-based bifunctional oxygen electrocatalysts. J Chin Chem Soc 66(8):829–865

14. Sohrabi S, Dehghanpour S, Ghalkhani M (2018) A cobalt porphyrin-based metal organic framework/multi-walled carbon nanotube composite electrocatalyst for oxygen reduction and evolution reactions. J Mater Sci 53(5):3624–3639
15. Wan H, Chen F, Ma W, Liu X, Ma R (2020) Advanced electrocatalysts based on two-dimensional transition metal hydroxides and their composites for alkaline oxygen reduction reaction. Nanoscale 12(42):21479–21496
16. Sun Y, Chen G, Xi S, Xu ZJ (2021) Catalytically influential features in transition metal oxides. ACS Catal 11(22):13947–13954
17. Ghalkhani M, Mirzaie RA, Banimostafa A (2020) Developing an efficient approach for preparation of cost-effective anode for ethanol oxidation reaction based on thin film electro-deposition of non-precious metal oxide. J Solid State Chem 288:121398
18. Morozan A, Jousselme B, Palacin S (2011) Low-platinum and platinum-free catalysts for the oxygen reduction reaction at fuel cell cathodes. Energy Environ Sci 4(4):1238–1254
19. Ghalkhani M, Gharagozlou M, Sohouli E, Khosrowshahi EM (2022) Preparation of an electrochemical sensor based on a HKUST-1/$CoFe_2O_4$/SiO_2-modified carbon paste electrode for determination of azaperone. Microchem J 175:107199
20. Sandhiran N, Ganapathy S, Manoharan Y, Ganguly D, Kumar M, Ramanujam K, Balachandran S (2022) CuO–NiO binary transition metal oxide nanoparticle anchored on rGO nanosheets as high-performance electrocatalyst for the oxygen reduction reaction. Environ Res 211:112992
21. Zhang H, Liu M, Cheng W, Li Y, Zhou W, Su H, Zhao X, Yao P, Liu Q (2019) Metallic Ni3N quantum dots as a synergistic promoter for nio nanosheet toward efficient oxygen reduction electrocatalysis. J Phys Chem C 123(14):8633–8639
22. Alegre C, Busacca C, Di Blasi O, Antonucci V, Aricò AS, Di Blasi A, Baglio V (2017) A combination of CoO and Co nanoparticles supported on electrospun carbon nanofibers as highly stable air electrodes. J Power Sources 364:101–109
23. Li J, Wang Q, Liu K, Jiang J, Qian D, Li J, Chen Z (2017) An extremely facile route to Co@CoO/N-RGO/AB with an enhanced electrocatalytic activity for ORR. Mater Lett 186:189–192
24. Niu Y, Huang X, Wu X, Zhao L, Hu W, Li CM (2017) One-pot synthesis of Co/N-doped mesoporous graphene with embedded Co/CoO_x nanoparticles for efficient oxygen reduction reaction. Nanoscale 9(29):10233–10239
25. Fu G, Yan X, Chen Y, Xu L, Sun D, Lee JM, Tang Y (2018) Boosting bifunctional oxygen electrocatalysis with 3D graphene aerogel-supported Ni/MnO particles. Adv Mater 30(5):1704609
26. Wu X, Gao X, Xu L, Huang T, Yu J, Wen C, Chen Z, Han J (2016) Mn_2O_3 doping induced the improvement of catalytic performance for oxygen reduction of MnO. Int J Hydrogen Energy 41(36):16087–16093
27. Sun M, Zhang G, Liu H, Liu Y, Li J (2015) α-and γ-Fe_2O_3 nanoparticle/nitrogen doped carbon nanotube catalysts for high-performance oxygen reduction reaction. Sci China Mater 58(9):683–692
28. Xiao Z, Hou F, Li Y, Zhang R, Shen G, Wang L, Zhang X, Wang Q, Li G (2019) Confinement of Fe_2O_3 nanoparticles in the shell of N-doped carbon hollow microsphere for efficient oxygen reduction reaction. Chem Eng Sci 207:235–246
29. Majidi MR, Farahani FS, Hosseini M, Ahadzadeh I (2019) Low-cost nanowired α-MnO_2/C as an ORR catalyst in air-cathode microbial fuel cell. Bioelectrochemistry 125:38–45
30. Worku AK, Ayele DW, Habtu NG, Yemata TA (2021) Engineering Co_3O_4/MnO_2 nanocomposite materials for oxygen reduction electrocatalysis. Heliyon 7(9):e08076
31. Zhang Y, Wang C, Fu J, Zhao H, Tian F, Zhang R (2018) Fabrication and high ORR performance of MnOx nanopyramid layers with enriched oxygen vacancies. Chem Commun 54(69):9639–9642
32. Li Z, Liu Z, Li B, Li D, Liu Z, Wang H, Li Q (2016) Large area synthesis of well-dispersed β-MnO_2 nanorods and their electrochemical supercapacitive performances. J Taiwan Inst Chem Eng 65:544–551
33. Cheng Y, Dou S, Veder J-P, Wang S, Saunders M, Jiang SP (2017) Efficient and durable bifunctional oxygen catalysts based on NiFeO@MnOx core–shell structures for rechargeable Zn–air batteries. ACS Appl Mater Interfaces 9(9):8121–8133
34. Xiao J, Wan L, Wang X, Kuang Q, Dong S, Xiao F, Wang S (2014) Mesoporous Mn_3O_4–CoO core–shell spheres wrapped by carbon nanotubes: a high performance catalyst for the oxygen reduction reaction and CO oxidation. J Mater Chem A 2(11):3794–3800
35. Tang C, Mao Y, Xie J, Chen Z, Tu J, Cao G, Zhao X (2018) $NiCo_2O_4$/MnO_2 core/shell arrays as a binder-free catalytic cathode for high-performance lithium–oxygen cells. Inorg Chem Front 5(7):1707–1713
36. Pakseresht S, Cetinkaya T, Al-Ogaili AWM, Akbulut H (2021) Urchin-like core-shell TiO_2/α-MnO_2 nanostructures as an active catalyst for rechargeable lithium-oxygen battery. Adv Powder Technol 32(3):895–907
37. Jiang L, Zhang G, Li D, Liu C, Xing S (2019) One-pot achievement of MnO_2/Fe_2O_3 nanocomposites for the oxygen reduction reaction with enhanced catalytic activity. New J Chem 43(43):16870–16875
38. Miao Q, Du Y, Wang G, Sun Z, Zhao Y, Zhang S (2019) In situ generated 3D hierarchical Co_3O_4@MnO_2 core–shell hybrid materials: self-assembled fabrication, morphological control and energy applications. J Mater Chem A 7(11):5967–5980
39. Li X, Xu N, Li H, Wang M, Zhang L, Qiao J (2017) 3D hollow sphere Co_3O_4/MnO_2-CNTs: its high-performance bi-functional cathode catalysis and application in rechargeable zinc-air battery. Green Energy Environ 2(3):316–328
40. Zhao H, Guo W (2021) Coordinated control method of multiple hybrid energy storage systems based on distributed event-triggered mechanism. Int J Electr Power Energy Syst 127:106637
41. Baghayeri M, Amiri A, Karimabadi F, Di Masi S, Maleki B, Adibian F, Pourali AR, Malitesta C (2021) Magnetic MWCNTs-dendrimer: a potential modifier for electrochemical evaluation of As(III) ions in real water samples. J Electroanal Chem 888:115059
42. Nodehi M, Baghayeri M, Kaffash A (2022) Application of BiNPs/MWCNTs-PDA/GC sensor to measurement of Tl(1) and Pb(II) using stripping voltammetry. Chemosphere 301:134701
43. Baghayeri M, Nabavi S, Hasheminejad E, Ebrahimi V (2022) Introducing an electrochemical sensor based on two layers of Ag nanoparticles decorated graphene for rapid determination of methadone in human blood serum. Top Catal 65:623–632

Publisher's Note Springer Nature remains neutral with regard to jurisdictional claims in published maps and institutional affiliations.

Springer Nature or its licensor (e.g. a society or other partner) holds exclusive rights to this article under a publishing agreement with the author(s) or other rightsholder(s); author self-archiving of the accepted manuscript version of this article is solely governed by the terms of such publishing agreement and applicable law.